Atomistic modeling of peptides bound to a chemically active surface: conformational implications‡

David Curcó,[a] Guillem Revilla-López,[b] Carlos Alemán[b,c]* and David Zanuy[b]*

This work presents a computational strategy to model flexible molecules tethered to a metallic rigid surface. The method is based on a previously developed procedure for inert surfaces, in which peptide–surface interactions were not considered. This procedure is able to generate uncorrelated relaxed microstructures at the atomistic level of systems containing relatively high densities of peptides tethered to the surface. The reliability of the strategy has been tested by simulating CREKA (Cys-Arg-Glu-Lys-Ala), a short linear pentapeptide that recognizes clotted plasma proteins and selectively homes to tumors, covalently tethered to a gold surface, results being compared with those obtained when the surface was represented as inert. The results indicate that the whole conformational profile of CREKA presents some correlation with the chemical activity of the surface, even though the bioactive conformation was found as the most favored in all cases. Specifically, simulations reflect that consideration of the peptide-surface interactions affect the geometrical orientation of the side chains, whereas the main chain conformation does not undergo significant modifications. Copyright © 2011 European Peptide Society and John Wiley & Sons, Ltd.

Keywords: computer simulations; conformational search; generation algorithm; metallic surface; tethered peptides; CREKA; tumor-homing peptides; peptide-surface interactions

Introduction

Nanotechnology approaches represent the ultimate frontier in diagnosis and treatment of diseases. Among different possible strategies, nanoparticle-based systems have taken the lead in tumor treatments [1–9]. Tumor chemical markers direct the nanoparticle-based device toward the malignant cells, being specially efficient if the molecular targets are receptors located in blood vessels grown around tumors [3–9]. In this context, the nanoparticles recently proposed by Ruoslahti *et al*. deserve special attention as they home to tumors amplifying their own homing activity by stimulating platelet clot formation [8]. These biomimetic nanoparticles were coated with a short linear peptide that recognizes clotted plasma proteins and selectively homes to tumors [8]. This peptide, with sequence Cys-Arg-Glu-Lys-Ala (CREKA, Cys-Arg-Glu-Lys-Ala), was recently discovered by *in vivo* screening of phage-display peptide libraries [4,10] for tumor homing in tumor-bearing MMTV-PyMT transgenic breast cancer mice [11]. CREKA peptide labeled with the fluorescent dye 5(6)-carboxyfluorescein (FMA) was detectable in human tumors from minutes to hours after intravenous injection, while it was essentially undetectable in normal tissues (Ruoslahti, personal communication (unpublished results)).

However, enhancement of the homing activity of peptides or improvement of their resistance toward proteolytic activity require explicit knowledge of their conformational preferences, in particular of the bioactive conformation/s. Experimental determination of the bioactive conformation is frequently a difficult task because of the peptide's inner flexibility. A feasible alternative is based on the use of computer simulation techniques, which allow us to explore the conformational preference of peptides and proteins.

Recently, we determined the bioactive conformation of CREKA using a multiple conformational search strategy based on MD simulations [12,13]. Calculations were performed using a simplified description of different experimentally tested environments. In one of these, a single CREKA molecule was bound to the surface of a nanoparticle, which was mimicked by attaching the sulfhydryl group of the Cys residue to the center of a square surface formed by 100 rigid van der Waals spherical particles (10 × 10). Clustering analyses of the results for this environment showed that the bioactive conformation of CREKA presents both a β-turn motif and strong electrostatic interactions involving the side chains of Arg, Glu and Lys [12,13]. These results were used to suggest the synthesis of different CREKA analogs based on the chemical modification of single residues, which led to improvement of the homing

* Correspondence to: Carlos Alemán and David Zanuy, Departament d'Enginyeria Química, E. T. S. d'Enginyers Industrials, Universitat Politècnica de Catalunya, Diagonal 647, 08028 Barcelona, Spain.
E-mail: carlos.aleman@upc.edu; david.zanuy@upc.edu

a Department d'Enginyeria Química, Facultat de Química, Universitat de Barcelona, Martí Franques 1, Barcelona E-08028, Spain

b Departament d'Enginyeria Química, E. T. S. d'Enginyers Industrials, Universitat Politècnica de Catalunya, Diagonal 647, 08028 Barcelona, Spain

c Center for Research in Nano-Engineering, Universitat Politècnica de Catalunya, Campus Sud, Edifici C', C/Pasqual i Vila s/n, Barcelona E-08028, Spain

‡ Special issue devoted to contributions presented at the E-MRS Symposium C "Peptide-based materials: from nanostructures to applications", 7–11 June 2010, Strasbourg, France.

peptide activity and to prove the turn shape of the bioactive conformation [14].

Despite the successful outcome of the bioactive conformation assessment, we were aware that a single-peptide molecule covalently tethered to a surface is a very rough description of a nanoparticle delivery system. For example, the nanoparticles used by Ruoslahti *et al.* were spherical (∼50 nm in diameter) and each one was coated by a large number of peptide molecules, i.e. around 8000 peptides per particle [8]. To improve the reliability of our molecular models and to overcome the serious limitations of atomistic MD simulations when dealing with surfaces with relatively high concentrations of flexible molecules covalently tethered (i.e. MD is very inefficient for dense systems as the motion of individual entities is easily hampered by steric hindrances), we recently developed a simple methodology to generate uncorrelated, energetically relaxed and representative structures [15].

The new method [15] consisted of a combination of an algorithm that generates representative atomistic microstructures of the coated surface, a procedure to construct energetically reliable configurations of the whole simulation box (including solvent molecules and ions, if present), and a relaxation method to minimize non-bonding interactions. We successfully investigated the conformation of CREKA peptides covalently tethered to a surface under diverse conditions, such as different density of peptides per $Å^2$ (ranged from 3×10^{-4} to 1.67×10^{-2}) or ionic strengths. Clustering analysis of the peptide conformations revealed that the structure identified as bioactive is the most stable and populated cluster in all cases. However, our initial approach was very simple and did not account for the interactions between the surface and the tethered molecules (i.e. the surface was considered as an inert element), even although they may play a major role in biasing the conformation of the peptides.

In this work, we present a significant improvement of this new methodology by introducing a chemical descriptor for the surface and considering the peptide–surface interactions in the construction and relaxation algorithms. The strategy allows us to describe active surfaces made of crystalline materials, such as metals, which are frequently used in nanomedicine. Moreover, the method can also be applied to other surfaces (e.g. clays and carbon – both graphite and diamond allotropic forms). The influence of the active surface on the peptide conformation has been examined on CREKA, results obtained in this work being compared with those reported for a completely inert surface [15]. However, it should be remarked that this is not intended to provide a deep and rigorous investigation of CREKA peptide, but to illustrate the potential utility of the new methodology in applications involving peptides attached to an active surface through a test case.

Theoretical Methodology

The principles followed in designing the generation, construction and relaxation algorithms were described in detail in our previous work [15]. Accordingly, in this section we only provide a brief background and describe the modifications that have been introduced to transform the inert surface into active.

The main steps followed in modeling the systems under study are summarized in Figure 1. The method consists of a three-step procedure. First, molecules tethered to the surface are
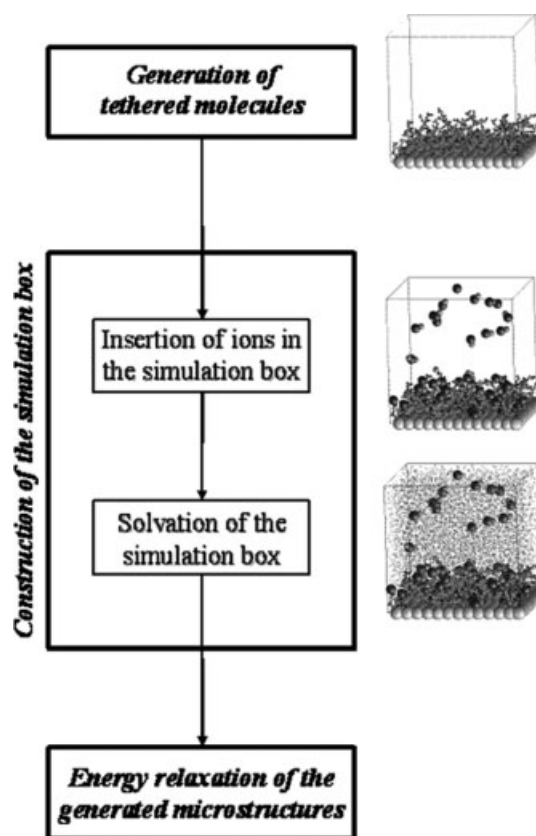

Figure 1. General flowchart of the theoretical strategy used to build peptides tethered to active surfaces.

generated without atomic overlaps or, in the case of systems with a very high density of molecules per $Å^2$, with atomic overlaps lower than a given threshold. In the second step, the simulation box is constructed by filling it with the counter-ions (in the case of charged molecules), solvent (if desired) and salt molecules (if the ionic strength is increased). To effectively eliminate the overlaps created in the first step for systems with a very high density of peptides per $Å^2$, the positions of the tethered molecules and the counter-ions are relaxed before filling the simulation box with explicit solvent molecules. Finally, the conformation and position of the molecules attached to the surface as well as the position of the ions and solvent molecules are relaxed.

Generation Algorithm

The generation algorithm is inspired in previously reported algorithms which provide atomistic models of amorphous polymers [16–18]. The positions of the atoms linked to the surface are randomly selected with the following restriction: the minimum distance between two of such atoms must be larger than $2.1 \cdot R$, R being the van der Waals radius. Each tethered chain is built following the strategy previously developed for comb-like polymers [17], which is based on two principles:

(1) The radii of atoms are reduced by multiplying them by a factor $\lambda < 1$. The use of scaled radii allows increase of computational efficiency, especially for dense systems, without any detriment to the reliability of the microstructures obtained at the end

of the process (i.e. unfavorable van der Waals interactions are easily relaxed).

(2) Atomic positions are generated residue-by-residue using a stochastic procedure. For each residue the backbone is generated before the side chain.

It should be noted that no definition of the peptide–surface interactions is required in this step. This is because the only energy evaluation performed during the generation of the peptide molecules, which is used to accept or reject atomic positions in (2) through a Monte Carlo (MC) criterion, is exclusively based on short-range interactions with the immediate neighbors.

Construction of the Simulation Box

The simulation box is filled using a two-step process. The first involves the insertion of both counter-ions and ions forming salt molecules, while the box is filled with solvent molecules in the second. The initial positions of the ions inside the simulation box are randomly selected but avoiding atomic overlaps with the previously generated peptides. These positions are further relaxed by applying random displacement moves, which are accepted if the energy of the configuration obtained after the displacement of the ion is lower than that of the configuration before such displacement. Before adding the solvent molecules, tethered peptides and ions are relaxed together, 80% of the moves corresponding to peptides. Finally, each solvent molecule is positioned at a position that produces attractive interaction energy with both the previously generated solvent molecules and the peptides. No scaling of the van der Waals radii is used in this algorithm.

In this case, the relaxation of both ions and peptides is performed considering the influence of the surface. For this purpose, the surface is parceled in a grid of points that represent the atom nuclei forming the ultra structure of the surface. The position of these points is equivalent to those atoms in the corresponding crystal structure. The grid of points defines the reference positions to calculate the interaction energy between the molecules located in the simulation box (i.e. peptides, solvent molecules and ions) and the surface. In this work, we have considered a metallic surface, the evaluation of the interaction energy being described through a conventional Lennard-Jones potential. Thus, the contribution of the surface is evaluated by computing atom pair distances between any particle in the simulation box and all the surface points that are within a previously defined cutoff distance.

Relaxation

The energy of the peptides tethered to the surface, the ions and the solvent molecules is minimized through a relaxation algorithm, which is applied using periodic boundary conditions at the *x*- and *y*-directions (i.e. those used to define the surface). To avoid an erroneous description of the system in the *z*-direction, the *c*-axis of the simulation box is divided into two different regions. All the solvent molecules contained in the simulation box that are placed below a specific distance to the *c*-axis edge are allowed to move during the relaxation process, whereas the solvent molecules above such distance are kept at fixed positions. Each relaxation cycle consists of the following three steps:

(1) The interaction energy is evaluated for each movable solvent molecule. The positions of the molecules with higher interaction energies are varied by introducing a random

displacement and a random rotation. The moves are accepted or rejected using a typical MC criterion.

(2) The positions of all the ions are improved by applying random displacements that are accepted when the energy decreases.

(3) The values of the dihedrals angles (90% of the moves) and the position (10% of the moves) of the tethered peptides are relaxed applying the same procedure that was used for the construction of the simulation box. The only difference is that in this case several randomly chosen dihedral angles move simultaneously.

As in the construction algorithm, the influence of the surface has been considered in the relaxation algorithm. The procedure used to define the position of the metallic atoms in the surface and the potential employed to define the interaction with all the particles contained in the simulation box were identical to those described above.

Molecular Models and Simulation Details

The theoretical strategy presented in this work was applied to explore the conformational space of CREKA peptides tethered to a metallic surface (see below) and surrounded by water molecules. In all cases the sulfur of the Cys was used to form the covalent linkage to the surface. The dimensions of the simulation box were $a = b = 60$ Å and $c = 90$ Å, where the regions along the *c*-axis defining the movable and fixed solvent molecules during the relaxation were defined by $c_1 = 60$ Å and $c_2 = 30$ Å, respectively. The MC criterion involved in the generation and relaxation algorithms was applied considering a temperature of 300 K.

The molecular model was built using the density of tethered CREKA peptides (σ, in peptides per Å^2) experimentally used by Roushlati *et al.*: $\sigma = 0.083$ peptides·Å^2, which is equivalent to 30 peptides attached to the surface. The system was completed with 90 counter-ions (30 Na$^+$ + 60 Cl$^-$) and 9621 water molecules. The chemical nature of the surface was represented using gold (Au), which is frequently used as sustaining metal for peptides.

The energy of the peptides was calculated using the following analytical potential function:

$$E = \sum_{\text{dihedrals}} \frac{V_n}{2}[1 + \cos(n\phi - \gamma)] + \sum_{\text{nonbonded}} \left[\frac{A_{ij}}{R_{ij}^{12}} - \frac{B_{ij}}{R_{ij}^6} + \frac{q_i q_j}{R_{ij}} \right]$$
(1)

where the first sum represents a series expansion for the torsional term followed by the Lennard-Jones and electrostatic terms. Non-bonding interactions of atoms connected by three atoms (1–4 interactions) were treated as in the AMBER force-field [19], applying a scaling factor of 0.5. The energy involving the solvent molecules and the ions was calculated using the non-bonding terms of Eqn (1), while the Lennard-Jones was the only term used to evaluate the interaction between the surface and the rest of species. Non-bonding interactions were evaluated using a cutoff of 14.0 Å. Force-field parameters for the CREKA peptide and the ions were taken from the AMBER libraries [19,20], while Optimized Potentials for Liquid Simulations (OPLS) van der Waals parameters for Au particles [21] were used to compute the interaction between the surface and the rest of species ($\sigma_{\text{Au}} = 1.789$ Å and $\varepsilon_{\text{Au}} = 0.193$ kcal·mol^{-1}). The Au nuclei were placed at the (100) lattice positions of a cubic F unit cell with crystallographic parameter $a = 2.93$ Å. Although this parameter is 1.4% larger

than the experimental one ($a = 2.89\,\text{Å}$), it was chosen for consistency with the van der Waals parameters of Au (i.e. this parameters predict that the closest distance is 2.93 Å) [21]. Finally, water molecules were represented using the TIP3P model [22]. Bond lengths and bond angles, which were also taken from the AMBER libraries [19] were kept fixed. A total of 1000 atomistic microstructures were generated and relaxed.

The results obtained for this system, hereafter denoted *Au-S/30*, have been compared with those previously obtained for an identical molecular model with exception of the surface [15], which was considered inert (i.e. the interaction between the surface and the rest of chemical species was neglected). In the next sections, the system with an inert surface has been denoted *Inert-S/30*. It should be noted that the computational resources required to simulate *Au-S/30* were one order or magnitude larger that those used for *Inert-S/30*, which were also significant due to large density of peptides per Å^2. This is because the number of interactions between atom pairs increased considerably when the surface participates in the construction and relaxation algorithms.

Influence of the Surface Nature on the Conformational Preferences

Figure 2 depicts the distribution of energies associated with the relaxed microstructures produced for *Au-S/30* and *Inert-S/30* models. The shape of the two distributions fits to a Gaussian function, which reflects the reliability of our theoretical approach. It is well known that the shape of the distribution of minima for a given model resembles a Gaussian function when the conformations can be described in terms of rotational isomers [23,24]. Although the width of the Gaussian function depends on the number of generated microstructures, such number was identical for the two surfaces under study. Furthermore, as was demonstrated in our previous studies on amorphous polymers [16–18], the generation method used in this work tends to provide representative microstructures rather than random ones. This feature guarantees that the left side of the Gaussian distribution is well described after generating a relatively low number of microstructures. The Boltzmann distributions displayed in Figure 2 clearly depend on the surface; the function becomes more narrow when the surface is allowed to interact with the chemical species contained in the simulation box. Thus, in general terms, it can
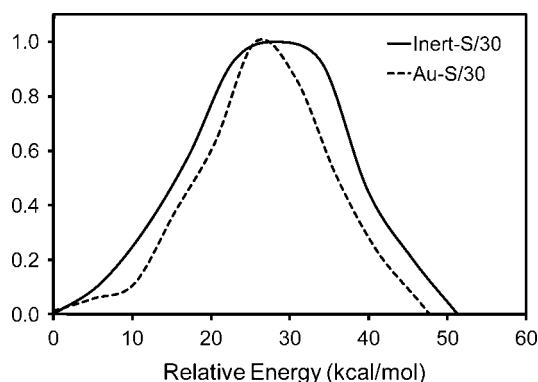
be stated that the conformational flexibility is smaller for *Au-S/30* than for *Inert-S/30*.

The conformational features of the CREKA peptide in *Au-S/30* and *Inert-S/30* models have been analyzed by considering each molecule as an independent case. A list of unique peptide conformations was constructed for each model by comparing all the molecules for all the produced microstructures. The list was organized by ranking all the unique peptide conformations according to their energies. Previously listed conformations were discarded from the list. A unique peptide conformation was identified if it did not share a set of selected structural parameters, which involve virtual backbone dihedral angles and intramolecular interactions. Virtual dihedral angles were defined considering the α-carbon atoms in the CREKA peptide, while the presence of polar interactions was accepted on the basis of geometric criteria: (i) hydrogen bonds: distance H–O shorter than 2.50 Å and angle $\angle$N–H–O larger than 120.0°, (b) salt bridges: distance between the geometric centers of the interacting groups shorter than 4.50 Å. The interaction pattern was also used to discriminate between side chain and main chain interacting groups. Two conformations were considered different if they differed at least in one virtual dihedral angle by more than 60° or in one of the interactions counted. For each model, all the conformations categorized as unique were clustered according to a criterion based on the presence of the interactions mentioned above: salt bridges and hydrogen bonds.

The number of unique conformations (clusters) and the percentage of structures present in each cluster for the two models are depicted in Figure 3. These percentages refer to the total amount of peptide conformations present in the 1000 microstructures (i.e. 30 peptides $\times$ 1000 microstructures $= 30\,000$ conformations) produced for the *Au-S/30* and *Inert-S/30* models. Figure 3 also includes the conformational preferences of a single CREKA molecule attached to a surface (hereafter referred to as *MD-S/1*), which were previously determined by MD simulations [12]. For this purpose, the results derived from such simulations have been clustered in this work using the procedure discussed above. The different environments in which CREKA was simulated led to a distribution of conformations with 45, 40 and 89 clusters for *Au-S/30, Inert-S/30* and *MD-S/1*, respectively, although only a small number of such clusters contained a significant number of structures. Specifically, the number of clusters that involve more than 1% of the total amount of conformations was 11, 16 and 20, respectively. Moreover, this number ranges from 2 to 5 if the threshold is increased to 10%. The results displayed in Figure 3 indicate that the conformation of CREKA is significantly restricted when the effects of the neighboring molecules, which are associated with the density of peptide per Å^2, are included in the model. However, independent of the nature of the surface, the results of the clustering are very similar, suggesting that the conformation of CREKA is dominated by the intramolecular interactions rather than by the intermolecular ones. Moreover, further analysis of each cluster shows that the conformation proposed as bioactive is predicted among the most favored ones independent of the characteristics of the surface (see below). However, significant differences have been observed depending on the activity of the surface as the *C*-termini of the peptides may be attracted by it.

The results presented in Figure 3 clearly narrow the conformational characterization of CREKA to the most representative clusters obtained for the different models. In the case of *Au-S/30* and *Inert-S/30*, more than 80% of the total amount of produced
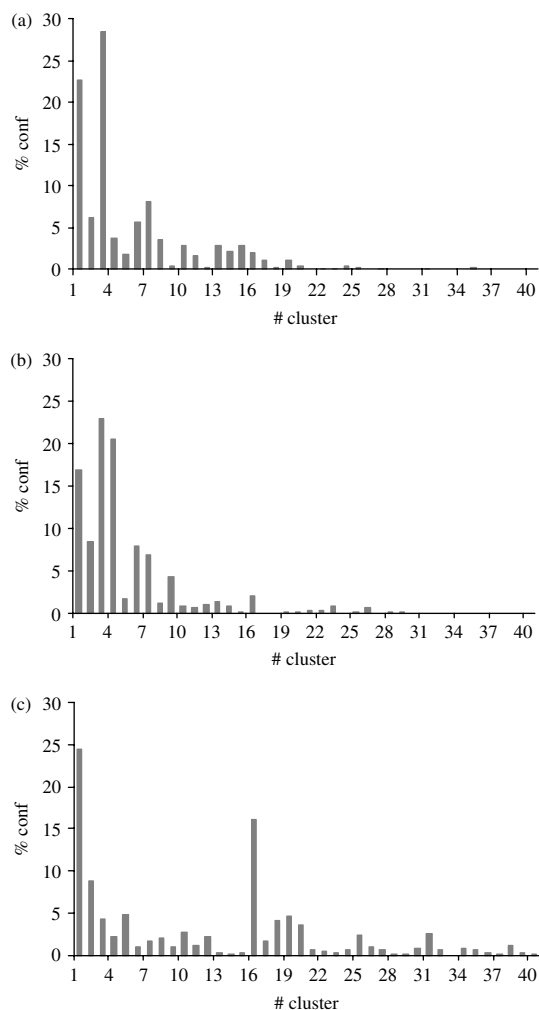

Figure 2. Normalized distribution of relative energies (in kcal/mol) for the microstructures of *Au-S/30* and *Inert-S/30* models obtained using the computational strategy presented in Figure 1.

Figure 3. Percentage of structures in each of the 40 and 45 clusters found in the simulation conditions corresponding to (a) *Inert-S/30* and (b) *Au-S/30*, respectively. Clusters are ordered considering the energy of the lead conformation (from the lowest to the highest), which corresponds to the most stable microstructure within the cluster. Results derived from MD simulations on a single CREKA molecule attached to a surface (Ruoslahti, personal communication (unpublished results)) are displayed in (c) for comparison (*MD-S/1* set in text).

Figure 4. Ramachandran plot distribution for the three central residues of CREKA, considering the most representative minimum energy structures for the *Inert-S/30* (black dots), *Au-S/30* (green dots) and *MD-S/1* (blue dots) models.

peptide conformations was clustered within the first seven clusters. The energy difference between the lead conformations of the most and least favored of such clusters was of only 3.0 kcal mol^{-1}. Accordingly, the most relevant conformational descriptors have been focused on those seven lead conformations. However, these results have been compared to the features observed using an isolated peptide tethered to a surface (*MD-S/1*). In the latter case, the first ten clusters concentrate 80% of the produced conformations.

Figure 4 depicts the Ramachandran plot of the Arg, Glu and Lys residues in the most populated clusters of *Au-S/30* and *Inert-S/30* models. As can be seen, most of the conformations cluster around a narrow region of the Ramachandran map, this feature being particularly evident for the Glu. Indeed, this trend was already described as one of most remarkable conformational characteristics of CREKA peptide, as the bioactive ensemble was based on tight-turns nucleated around Glu residue [12]. However, the conformational preferences of *MD-*
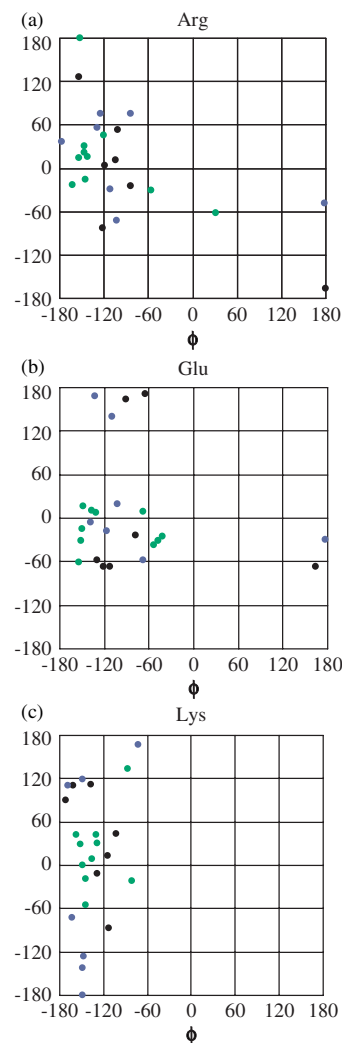
S/1 are similar to those of *Au-S/30* and *Inert-S/30*, suggesting again that the conformational preferences exhibited by the central segment of CREKA are driven by intramolecular interactions. For the three studied systems the most relevant differences are found at the *C*-termini of the peptide (Lys), while the central core (Arg and Glu) tends to present very low conformational variability (i.e. the φ, ψ values observed for *Au-S/30* and *Inert-S/30* are close to those obtained for *MD-S/1*).

In spite of Figure 4 suggesting that the conformational preferences of the CREKA are independent of the surface, there are some differences among the conformations produced for *Au-S/30* and *Inert-S/30* that deserve consideration. The organizations obtained for the *C*-termini of the peptide when the surface participates or not in the interaction energy are significantly different. Thus, in *Au-S/30* the edge of the peptide that is far from the group directly tethered to the surface (i.e. Cys side chain) is able to bend, interacting not only with other peptide chains but also with the surface itself. Accordingly, the metallic surface partially affects the conformational properties of the tethered peptides.
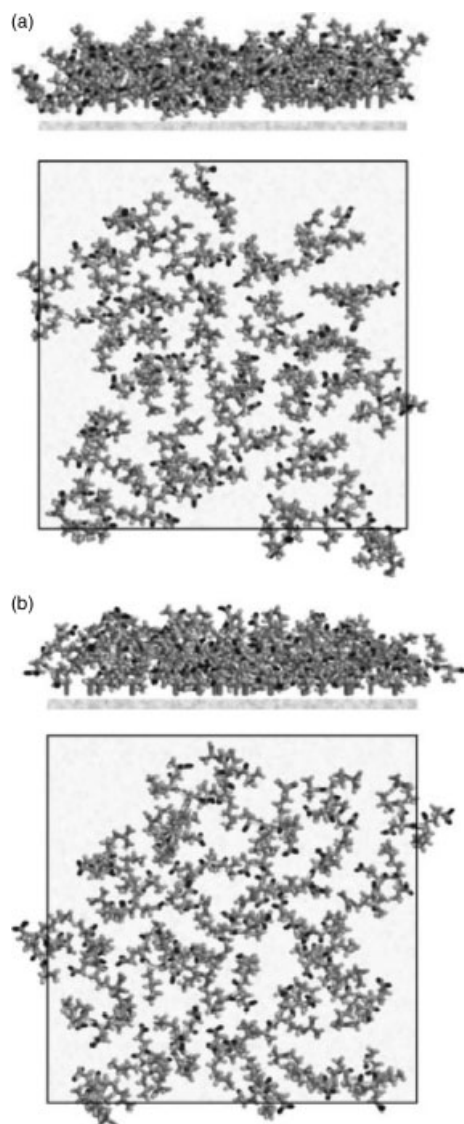
Figure 5. Axial (top panels) and equatorial (bottom panels) projections of a representative microstructure for the (a) *Au-S/30* and (b) *Inert-S/30* models. Ions, solvent molecules and the *c*-axis have been omitted to clarify the picture.

Figure 6. Conformational correlation expressed through the RMSD of the backbone atoms for the most representative conformations produced for the three models. Filling colors represent different degrees of similarity referred to the value of RMSD: less than 1.3 Å green; higher than 1.3 Å and lower than 2.0 Å white; higher than 2.0 Å and lower than 3.0 Å orange; and higher than 3.0 Å red. The labels NA#, A# and WT# refer to the conformations of the more populated clusters produced for *Inert-S/30, Au-S/30* and *MD-S/1*, respectively.

Specifically, unspecific peptide–surface van der Waals interactions induce chains to move away when the intrinsic conformational tendencies of the peptides allow them to bend and intermolecular interactions do not reduce their flexibility (Figure 5(a)). In contrast, the lack of peptide–surface interactions facilitates that a large amount of molecules lay on the surface of the simulated barrier, as is reflected in Figure 5(b) for *Inert-S/30*. However, it should be emphasized that for *Au-S/30* the interactions with the surface are not strong enough to revert decisively the intrinsic conformational preferences of the peptide core, as is evidenced in Figure 4 for the Arg and Glu residues.

To extend the analysis over the conformational particularities of each studied model, the structural correlation among all the low energy conformations has been established. Thus, the produced conformations have been compared transversally, beyond the theoretical methodology used to obtain them or the characteristics of the surface. Specifically, the backbone root mean square deviation (RMSD) of the last four residues has been computed for all
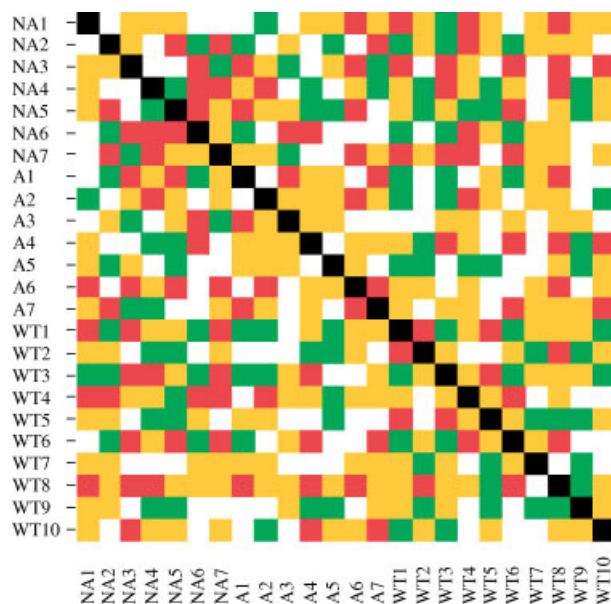
possible pairs of conformations. The results of this analysis, which are plotted in Figure 6, confirm the influence of the surface activity in the more favored arrangements of the peptide molecules. Thus, inspection of the similarities among the different models indicates that, in general, the conformations obtained for *MD-S/1* are closer to those produced for *Au-S/30* than for *Inert-S/30*. The *Au-S/30* conformations present 48% of the computed chain pair RMSDs below 2.0 Å, whereas this percentage reduces to 35% for the *Inert-S/30* conformations. As it was mentioned above, the *MD-S/1* model allowed consider peptide–surface interactions through a surface descriptor (i.e. the spheres used to define the nanoparticle were allowed to interact with the peptide molecule through a Lennard-Jones potential, even though they did not represent any realistic material) [12]. Accordingly, the two models with active surfaces reached similar molecular conformations, even though the molecular environments were different (i.e. isolation and high density of molecules per Å^2 for *MD-S/1* and *Au-S/30*, respectively).

Conclusions

The previously developed strategy has been extended by including a potential that describes the attractive and repulsive interactions between the surface and the rest of chemical species in the construction and relaxation algorithms. The surface descriptor is based on a grid of points that represents the geometrical organization of atoms or molecules in a crystalline structure. Accordingly, the new strategy is able to produce energetically representative structures of flexible peptides tethered to a surface with chemical identity. Although the description of the systems modeled using this new procedure is more realistic, the computational resources required for simulations also increase significantly.

To examine the influence of the surface activity on the conformational preferences of peptide, a system formed by 30 CREKA molecules covalently linked to an Au surface of 60×60 Å^2 has been simulated using this new strategy. Results have been compared with those obtained for (i) a system with identical chemical composition with exception of the surface, which is not able to interact with peptides, solvent molecules or ions (i.e. inert surface), and (ii) a system formed by a single-peptide molecule attached to a van der Waals surface, which was previously studied using conventional MD simulations.

Analysis of the results indicates that the omission of the chemical definition of the surface produce spatial arrangements for the peptides that might preclude the proper organization of the side chains. Specifically, the Au surface affects the orientation of the CREKA molecules by influencing the conformation of the edge residues and the subsequent organization of the ionized side chains. Even though the intrinsic preferences of the peptide main chain remain practically unaltered by the active surface, a proper description of the ionized side chains requires a reliable definition of the interactions with the surface. Thus, an erroneous representation of the ionized side chains organization would lead to a misunderstanding of the nanoparticle function hampering potential further chemical improvements.

References

1 Weissleder R, Bogdanov A Jr, Neuwelt EA, Papisov M. Long-circulating iron oxides for MR imaging. *Adv. Drug Delivery Rev.* 1995; **16**: 321–334.

2 Sinek J, Frieboes H, Zheng X, Cristini V. Two-dimensional chemo-therapy simulations demonstrate fundamental transport and tumor response limitations involving nanoparticles. *Biomed. Microdevices* 2004; **6**: 297–309.

3 Hoffman JA, Giraudo E, Singh M, Zhang L, Inoue M, Porkka K, Hanahan D, Ruoslahti E. Progressive vascular changes in a transgenic mouse model of squamous cell carcinoma. *Cancer Cell* 2003; **4**: 383–391.

4 Oh P, Li Y, Yu J, Durr E, Krasinska KM, Carver LA, Testa JE, Schnitzer JE. Substractive proteomic mapping of the endothelial surface in lung and solid tumors for tissue-specific therapy. *Nature* 2004; **429**: 629–635.

5 Ruoslahti E. Specialization of tumour vasculature. *Nat. Rev. Cancer* 2002; **2**: 83–90.

6 Akerman ME, Chan WC, Laakkonen P, Bhatia SN, Ruoslahti E. Nano-crystal targeting in vivo. *Proc. Natl. Acad. Sci. U.S.A.* 2002; **99**: 12617–12621.

7 Cai W, Shin DW, Chen K, Gheysens O, Cao Q, Wang SX, Gambhir SS, Chen X. Peptide-labeled near-infrared quantum dots for imaging tumor vasculature in living subjects. *Nano Lett.* 2006; **6**: 669–676.

8 Simberg D, Duza T, Park JH, Essler M, Pilch J, Zhang L, Derfus AM, Yang M, Hoffman RM, Bhatia S, Sailor MJ, Ruoslahti E. Biomimetic amplification of nanoparticle homing to tumors. *Proc. Natl. Acad. Sci. U.S.A.* 2007; **104**: 932–936.

9 Riehemann K, Schneide SW, Luger TA, Godin B, Ferrari M, Fuchs H. Nanomedicine–challenge and perspectives. *Angew. Chem., Int. Ed. Engl.* 2009; **48**: 872–897.

10 Pasqualini R, Ruoslahti E. Organ targeting in vivo using phage display peptide libraries. *Nature* 1996; **380**: 364–366.

11 Hutchinson JN, Muller WJ. Transgenic mouse models of human breast cancer. *Oncogene* 2000; **19**: 6130–6137.

12 Zanuy D, Flores-Ortega A, Casanovas J, Curcó D, Nussinov R, Alemán C. The energy landscape of a selective tumor-homing pentapeptide. *J. Phys. Chem. B* 2008; **112**: 8692–8700.

13 Zanuy D, Curcó D, Nussinov R, Alemán C. Influence of the dye presence on the conformational preferences of CREKA, a tumor homing linear pentapeptide. *Biopolymers* 2009; **90**: 83–93.

14 Agemy L, Sugahara KN, Kotamraju VR, Gujraty K, Girard OM, Kono Y, Mattrey RF, Park JH, Sailor M, Jimenez AI, Cativiela C, Zanuy D, Sayago FJ, Aleman C, Nussinov R, Ruoslahti E. Nanoparticle-induced vascular blockade in human prostate cancer. *Blood* 2010; in press. DOI: 10.1182/blood-2010-03-274258.

15 Curcó D, Zanuy D, Nussinov R, Alemán C. A simulation strategy for the atomistic modeling of flexible molecules covalently tethered to rigid surfaces: application to peptides. *J. Comput. Chem.* 2010; in press. DOI: 10.1002/jcc.21647.

16 Curcó D, Alemán C. Simulation of dense amorphous polymers by generating representative atomistic models. *J. Chem. Phys.* 2003; **119**: 2915–2922.

17 Curcó D, Alemán C. A theoretical strategy to provide atomistic models of comblike polymers: a generation algorithm combined with configurational bias Monte Carlo. *J. Chem. Phys.* 2004; **121**: 9744–9752.

18 Curcó D, Alemán C. A computational tool to model the packing of polycyclic chains: structural analysis of amorphous polythiophene. *J. Comput. Chem.* 2007; **28**: 1743–1749.

19 Wang J, Cieplak P, Kollman PA. How well does a restrained electrostatic potential (resp) model perform in calculating conformational energies of organic and biological molecules. *J. Comput. Chem.* 2000; **21**: 1049–1074.

20 Cornell WD, Cieplak P, Bayly CI, Gould IR, Merz KM, Ferguson DM, Spellmeyer DC, Fox T, Caldwell JW, Kollman P. A second generation force field for the simulation of proteins, nucleic acids, and organic molecules. *J. Am. Chem. Soc.* 1995; **117**: 5179–5197.

21 Iori F, Di Felice R, Molinari E, Corni S. GolP: an atomistic force-field to describe the interaction of proteins with Au(111) surfaces in water. *J. Comput. Chem.* 2009; **30**: 1465–1476.

22 Jorgensen WL, Chandrasekhar J, Madura JD, Impey RW, Klein ML. Comparison of simple potential functions for simulating liquid water. *J. Chem. Phys.* 1983; **79**: 926–935.

23 Pérez JJ, Villar HO, Loew GH. Characterization of low-energy conformational domains for Met-enkephalin. *J. Comput.-Aided Mol. Des.* 1992; **6**: 175–190.

24 Pérez JJ, Villar HO, Arteca GA. Distribution of conformational energy minima in molecules with multiple torsional degrees of freedom. *J. Phys. Chem.* 1994; **98**: 2318–2324.